energy&fuels

Article

pubs.acs.org/EF

Assessment of Variability in the Thermophysical Properties of Rocket Propellant RP-1

Tara J. Fortin*

National Institute of Standards and Technology, Material Measurement Laboratory, Thermophysical Properties Division, 325 Broadway MS 838.07, Boulder, Colorado 80305, United States

ABSTRACT: Density, speed of sound, and viscosity have been measured for 11 orthogonal blends of the rocket propellant RP-1. Density and speed of sound were measured over the temperature range of 278 to 343 K, while viscosity was measured from 263 to 373 K. All measurements were made at ambient atmospheric pressure. The density and sound speed data were used to derive adiabatic compressibilities, and those results are also reported. Different, yet significant, degrees of variability over the 11 RP-1 samples were observed for all reported properties. The largest variability was observed for viscosity. The measurement data were also compared to previously reported results for an additional RP-1 sample and to the predictions of an existing surrogate mixture model. Discrepancies were observed that seem to indicate a need for the development of a more general model to capture the whole range of thermophysical property variability that is possible with the RP-1 fuel.

INTRODUCTION

The liquid propellant rocket engine (LPRE) was conceived of over 100 years ago, but it was Robert H. Goddard who is credited with both the first actual construction of and the first flight of an LPRE in 1921 and 1926, respectively.[1] For that flight, Goddard used gasoline as the fuel and liquid oxygen (LOX) as the oxidizer. Since then, various other fuels have been utilized in different combinations, depending on the specific application. In fact, an estimated 170 different fuels have undergone laboratory evaluations as potential liquid propellants.[1,2] Every choice of propellant combination is ultimately a compromise between desirable qualities such as high density, low cost, and long-term storage stability, and undesirable qualities such as corrosivity, flammability, and toxicity.[1] However, after more than 50 years of operational experience, certain propellants and propellant combinations have proven themselves to be most useful in U.S. space applications; these include hydrazine (as a monopropellant), nitrogen tetroxide/hydrazine, liquid hydrogen (LH2)/LOX, kerosene/peroxide, and kerosene/LOX.[1,3]

Kerosene is obtained from the fractional distillation of petroleum between approximately 200 and 300 °C.[3] Because jet fuels are kerosenes, they were utilized as the initial kerosenes for rocket tests. However, it became clear that the physical property specifications for jet fuels (e.g., their chemical components, density, volatility, etc.) were not sufficiently tight for them to be effective rocket propellants. That problem was ultimately overcome in the mid-1950s with the development of rocket propellant 1 (RP-1).[3] Compared to common jet fuels, RP-1 specifications allow for a narrower density range and lower concentrations of certain fuel components thought to cause deposits during regenerative cooling (e.g., sulfur, olefins, and aromatics).[4] Specifically, density is allowed to vary from 0.799 to 0.815 g/cm^3, and the maximum allowed sulfur, olefin, and aromatic concentrations are limited to 30 mg/kg, 2.0% vol/vol, and 5.0% vol/vol, respectively.[5]

Typically, RP-1 is formulated by mixing together different blending stocks according to established formulas to produce a fuel that meets specifications. Despite the strictness of those specifications, there have been indications that some engine manufacturers and launch service providers have encountered an unanticipated degree of variability among RP-1 formulations.[6−8] In an effort to evaluate the possible range of compositional variability and the resultant consequences for the fuel's thermophysical properties, a comprehensive study was undertaken at the National Institute of Standards and Technology (NIST). As part of that study, Lovestead et al. recently reported their assessment of the compositional variability as determined by the advanced distillation curve method.[9] In this paper, measurements made at ambient pressure of the thermophysical properties density, speed of sound, and viscosity are reported.

MATERIALS AND METHODS

A total of 11 separate samples of RP-1 were obtained for this work. Each sample was independently prepared using a distinct recipe while still meeting existing fuel specifications.[5] Furthermore, the 11 samples were considered to be orthogonal. In other words, samples were prepared in a manner that ensured there was no correlation or interrelation between samples. Specifically, orthogonal samples are free from carryover or correlation that can occur between batches that are sequentially added to a storage tank. Furthermore, the orthogonal samples were specifically formulated to reflect the full range of variability that could reasonably be encountered with RP-1. All samples were pink in color due to the presence of the dye additive azobenzene-4-azo-2-naphthol. The chemical composition of each sample was previously analyzed using gas chromatography−mass spectrometry (GC−MS),[10,11] and the results were reported by Lovestead et al.[9] For each of the 11 samples, a subset of the more than 60 reported components is shown in Table 1. Specifically, the top 10 components and their corresponding CAS registry numbers are listed, sorted by the uncalibrated area percent. For each RP-1 sample, the components listed in Table 1 account for approximately 35−42% of the total reported area. As Table 1 shows, the RP-1 samples are composed primarily of linear and branched alkanes (or paraffins) up to C21 (2,6,10,15-tetramethylheptadecane),

Received: March 5, 2012
Revised: May 18, 2012
Published: June 14, 2012

Table 1. Top 10 Components (by Area %) of the 11 RP-1 Samples

compound	CAS no.	area %
Blend 1		
n-dodecane	112-40-3	4.02
n-tetradecane	629-59-4	3.55
n-tridecane	629-50-5	2.98
2,6-dimethylundecane	17301-23-4	2.95
2-methylundecane	7045-71-8	2.42
2-methyl decalin	2958-76-1	2.34
5-methylundecane	1632-70-8	2.06
3-methylundecane	1002-43-4	2.00
2,3,6-trimethyloctane	62016-33-5	1.87
cis-decalin	42588-37-2	1.77
Blend 2		
2,6-dimethylundecane	17301-23-4	3.00
2-methyl decalin	2958-76-1	2.40
2,3,6-trimethyloctane	62016-33-5	2.20
n-dodecane	112-40-3	2.00
2-methylundecane	7045-71-8	1.90
2,10-dimethylundecane	17301-27-8	1.90
5-methylundecane	1632-70-8	1.80
n-tetradecane	629-59-4	1.80
hexylcyclohexane	4292-75-5	1.70
trans-decalin	493-02-7	1.60
Blend 3		
2-methyl decalin	2958-76-1	2.65
2,6-dimethylundecane	17301-23-4	2.47
n-dodecane	112-40-3	2.00
2-methylundecane	7045-71-8	1.96
5-methylundecane	1632-70-8	1.92
trans-decalin	493-02-7	1.91
2,6-dimethylnonane	17302-28-2	1.81
2,3,6-trimethyloctane	62016-33-5	1.76
cis-decalin	42588-37-2	1.72
n-undecane	1120-12-4	1.60
Blend 4		
2,6-dimethylundecane	17301-23-4	3.75
2,3,6-trimethyloctane	62016-33-5	2.60
n-dodecane	112-40-3	2.41
2-methyl decalin	2958-76-1	2.38
2-methylundecane	7045-71-8	2.35
2,10-dimethylundecane	17301-27-8	2.06
4-methylundecane	2980-69-0	2.02
5-methylundecane	1632-70-8	2.01
3-methylundecane	1002-43-4	2.00
trans-2-methyl decalin	100015-24-7	1.98
Blend 5		
2,6-dimethylundecane	17301-23-4	3.22
2-methyl decalin	2958-76-1	2.61
2,*y*,*z*-trimethyldodecane[a]		2.23
2,3,6-trimethyloctane	62016-33-5	2.21
2-methylundecane	7045-71-8	2.08
5-methylundecane	1632-70-8	1.87
2,10-dimethylundecane	17301-27-8	1.73
trans-2-methyl decalin	100015-24-7	1.73
3-methyltridecane	6418-41-3	1.72
3-methylundecane	1002-43-4	1.70
Blend 6		
2,6-dimethylundecane	17301-23-4	3.53
2-methylundecane	7045-71-8	2.36
2,3,6-trimethyloctane	62016-33-5	2.35
2-methyl decalin	2958-76-1	2.33
n-dodecane	112-40-3	2.31

compound	CAS no.	area %
Blend 6		
5-methylundecane	1632-70-8	2.18
hexylcyclohexane	4292-75-5	2.00
2,10-dimethylundecane	17301-27-8	1.92
2,6-dimethyl decalin	1618-22-0	1.91
4-methylundecane	2980-69-0	1.89
Blend 7		
n-tridecane	629-50-5	3.23
n-dodecane	112-40-3	2.84
2,6-dimethylundecane	17301-23-4	2.33
n-tetradecane	629-59-4	2.03
2,3,6-trimethyloctane	62016-33-5	1.94
2,6,10,15-tetramethylheptadecane	54833-48-6	1.94
2,*y*,*z*-trimethyldodecane[a]		1.85
2,10-dimethylundecane	17301-27-8	1.68
2-methyl decalin	2958-76-1	1.62
3-methylundecane	1002-43-4	1.52
Blend 8		
2,6-dimethylundecane	17301-23-4	2.59
2-methyl decalin	2958-76-1	2.30
adamantane	281-23-2	2.18
2,*y*,*z*-trimethyldodecane[a]		2.18
2,6,10,15-tetramethylheptadecane	54833-48-6	2.18
x,*y*-dimethylundecane[a]		2.02
2-methylundecane	7045-71-8	1.76
5-methylundecane	1632-70-8	1.70
3-methyltridecane	6418-41-3	1.69
2,10-dimethylundecane	17301-27-8	1.58
Blend 9		
n-dodecane	112-40-3	4.38
n-tridecane	629-50-5	3.00
n-undecane	1120-12-4	2.70
n-tetradecane	629-59-4	2.25
2,6-dimethylundecane	17301-23-4	2.21
3-methylundecane	1002-43-4	2.08
2,*y*,*z*-trimethyldodecane[a]		1.85
2-methylundecane	7045-71-8	1.78
3-methyltridecane	6418-41-3	1.74
5-methylundecane	1632-70-8	1.73
Blend 10		
n-undecane	1120-12-4	3.50
n-dodecane	112-40-3	2.92
2,6,10,15-tetramethylheptadecane	54833-48-6	2.26
2,6-dimethylundecane	17301-23-4	2.09
2,3,6-trimethyloctane	62016-33-5	1.83
3-methyltridecane	6418-41-3	1.73
2-methyl decalin	2958-76-1	1.71
2,10-dimethylundecane	17301-27-8	1.61
5-methylundecane	1632-70-8	1.60
2-methylundecane	7045-71-8	1.56
Blend 11		
2,6-dimethylundecane	17301-23-4	2.42
2-methyl decalin	2958-76-1	2.31
n-dodecane	112-40-3	2.00
2,6,10,15-tetramethylheptadecane	54833-48-6	1.98
2,3,6-trimethyloctane	62016-33-5	1.79
2,*y*,*z*-trimethyldodecane[a]		1.75
5-methylundecane	1632-70-8	1.74
2-methylundecane	7045-71-8	1.71
3-methyltridecane	6418-41-3	1.59
2,10-dimethylundecane	17301-27-8	1.55

[a]Note that it is not always possible to determine the position of the methyl substitution, and in these instances the position is indicated with a letter rather than a number.

dx.doi.org/10.1021/ef3004009 | *Energy Fuels* 2012, 26, 4383−4394

Table 2. Densities of the 11 RP-1 Samples Measured in the Density and Sound Speed Analyzer at Ambient Pressure[a]

T (K)	Blend 1 $\bar{\rho}$ (kg m^{-3})	Blend 1 $U(\bar{\rho})$ (kg m^{-3})	Blend 2 $\bar{\rho}$ (kg m^{-3})	Blend 2 $U(\bar{\rho})$ (kg m^{-3})	Blend 3 $\bar{\rho}$ (kg m^{-3})	Blend 3 $U(\bar{\rho})$ (kg m^{-3})	Blend 4 $\bar{\rho}$ (kg m^{-3})	Blend 4 $U(\bar{\rho})$ (kg m^{-3})	Blend 5 $\bar{\rho}$ (kg m^{-3})	Blend 5 $U(\bar{\rho})$ (kg m^{-3})	Blend 6 $\bar{\rho}$ (kg m^{-3})	Blend 6 $U(\bar{\rho})$ (kg m^{-3})
343.15	770.82	0.06	773.45	0.06	769.28	0.06	772.38	0.06	775.88	0.06	771.90	0.06
338.15	774.50	0.06	777.12	0.06	772.96	0.06	776.06	0.06	779.53	0.06	775.58	0.06
333.15	778.17	0.06	780.77	0.06	776.63	0.06	779.73	0.06	783.18	0.06	779.25	0.06
328.15	781.83	0.06	784.41	0.06	780.29	0.06	783.38	0.06	786.81	0.06	782.92	0.06
323.15	785.48	0.06	788.05	0.06	783.93	0.06	787.03	0.06	790.44	0.06	786.57	0.06
318.15	789.13	0.06	791.68	0.06	787.58	0.06	790.68	0.06	794.06	0.06	790.22	0.06
313.15	792.77	0.06	795.31	0.06	791.21	0.06	794.31	0.06	797.68	0.06	793.86	0.06
308.15	796.41	0.06	798.93	0.06	794.84	0.06	797.94	0.06	801.29	0.06	797.49	0.06
303.15	800.03	0.06	802.55	0.06	798.47	0.06	801.57	0.06	804.89	0.06	801.13	0.06
298.15	803.65	0.06	806.16	0.06	802.10	0.07	805.19	0.06	808.50	0.06	804.75	0.06
293.15	807.27	0.06	809.76	0.06	805.75	0.08	808.81	0.06	812.10	0.06	808.38	0.06
288.15	810.89	0.06	813.37	0.06	809.41	0.10	812.43	0.06	815.70	0.06	812.00	0.06
283.15	814.51	0.06	816.97	0.06	813.07	0.12	816.05	0.06	819.30	0.06	815.62	0.06
278.15	818.13	0.06	820.58	0.06	816.73	0.14	819.67	0.06	822.90	0.06	819.24	0.06

T (K)	Blend 7 $\bar{\rho}$ (kg m^{-3})	Blend 7 $U(\bar{\rho})$ (kg m^{-3})	Blend 8 $\bar{\rho}$ (kg m^{-3})	Blend 8 $U(\bar{\rho})$ (kg m^{-3})	Blend 9 $\bar{\rho}$ (kg m^{-3})	Blend 9 $U(\bar{\rho})$ (kg m^{-3})	Blend 10 $\bar{\rho}$ (kg m^{-3})	Blend 10 $U(\bar{\rho})$ (kg m^{-3})	Blend 11 $\bar{\rho}$ (kg m^{-3})	Blend 11 $U(\bar{\rho})$ (kg m^{-3})
343.15	773.57	0.06	773.27	0.06	765.00	0.06	770.07	0.06	771.34	0.06
338.15	777.22	0.06	776.93	0.06	768.68	0.06	773.72	0.06	775.00	0.06
333.15	780.86	0.06	780.58	0.06	772.34	0.06	777.35	0.06	778.64	0.06
328.15	784.49	0.06	784.22	0.06	775.99	0.06	780.97	0.06	782.28	0.06
323.15	788.11	0.06	787.85	0.06	779.63	0.06	784.59	0.06	785.91	0.06
318.15	791.72	0.06	791.47	0.06	783.27	0.06	788.20	0.06	789.54	0.06
313.15	795.34	0.06	795.09	0.06	786.90	0.06	791.80	0.06	793.15	0.06
308.15	798.95	0.06	798.70	0.06	790.52	0.06	795.41	0.06	796.77	0.06
303.15	802.55	0.06	802.31	0.06	794.14	0.06	799.00	0.06	800.38	0.06
298.15	806.15	0.06	805.92	0.06	797.76	0.07	802.59	0.06	803.99	0.06
293.15	809.75	0.06	809.52	0.06	801.38	0.08	806.18	0.06	807.60	0.06
288.15	813.35	0.06	813.12	0.06	805.01	0.10	809.77	0.06	811.24	0.08
283.15	816.95	0.06	816.72	0.06	808.64	0.12	813.36	0.06	814.89	0.10
278.15	820.55	0.06	820.32	0.06	812.28	0.13	816.95	0.07	818.55	0.15

[a]Ambient pressure during measurements was ~83 kPa.

although 7 of the 11 samples also contain a small amount (<0.12 area %) of tetratetracontane (C44). According to the hydrocarbon classification[12,13] reported by Lovestead el al.,[9] paraffins account for approximately 32−39%, by volume, of the total composition for these samples. In addition to the paraffins, the RP-1 samples also contain a significant number of cycloalkanes (or cycloparaffins); approximately 34−40% and 17−25%, by volume, of the total composition are made up of monocycloparaffins and dicycloparaffins, respectively.[9] Finally, in addition to the paraffins and cycloparaffins, the RP-1 samples also contain a small amount of aromatics.

A commercial density and sound speed analyzer, the DSA 5000 from Anton Paar, was used to simultaneously measure these two properties over the temperature range 278 to 343 K and at ambient pressure (~83 kPa in Boulder, CO). (In order to describe materials and experimental procedures adequately, it is occasionally necessary to identify commercial products by manufacturers' names or labels. In no instance does such identification imply endorsement by the National Institute of Standards and Technology nor does it imply that the particular product or equipment is necessarily the best available for the purpose). The speed of sound is measured using a time-of-flight technique. The sound speed cell consists of a circular cylindrical cavity (8 mm diameter and 5 mm thick) that is sandwiched between two piezoelectric ultrasound transducers. One transducer acts as the transmitter sending sound pulses through the sample-filled cavity at a frequency of approximately 3 MHz; the second transducer then receives those pulses. Speed of sound (w) is ultimately determined by measuring the propagation time between the transmitter and receiver. The densimeter employs the vibrating-tube method where density (ρ) is derived from the resonant frequency of a sample-filled U-shaped tube as it vibrates perpendicular to its plane in an electromagnetic field. The resonator in this instrument is constructed of borosilicate glass. The sound speed cell and the density cell are both housed in a thermostated copper block whose temperature is controlled with a combination of thermoelectric Peltier elements and an integrated Pt-100 resistance thermometer. Measurements of air and water performed at 293 K, 313 K, and 333 K are required to adjust the apparatus constants in the instrument's working equations for both sound speed and density; this is referred to as an adjustment procedure. Additionally, regular calibration measurements are performed to verify the instrument's performance between adjustment procedures. Our calibration procedure involves measuring water and toluene standard reference material (SRM) 211d[14] every 5 K from 343 to 278 K. Additional details about the density and sound speed analyzer can be found in Fortin et al.[15] and Laesecke et al.[16]

A commercial viscodensimeter, the SVM 3000 from Anton Paar, was used to simultaneously measure viscosity and density over the temperature range 263 to 373 K and at ambient pressure. Density is measured with a vibrating-tube densimeter made of borosilicate glass. Viscosity is measured with a Stabinger rotating concentric cylinder viscometer. The horizontally mounted outer cylinder is made of Hastelloy, while the inner cylinder is made of titanium. The inner cylinder contains a small magnet but is otherwise hollow. When sample is injected into the cell, it fills the annular gap between the inner and outer cylinders. During measurements, the outer cylinder is rotated at 3500 rpm by an external electric motor, and the inner cylinder is dragged into rotation by the rotating sample liquid. The revolutions of the rotating field of the magnet in the inner cylinder are measured with a Hall effect sensor, and the dynamic viscosity (η) is ultimately obtained from the ratio of the number of revolutions of the

outer and inner cylinders. Both the density and viscosity measurement cells are housed in a thermostated copper block whose temperature is controlled between 273 and 373 K with a combination of thermoelectric Peltier elements and an integrated Pt-100 resistance thermometer. The addition of an external circulating bath extends the instrument's temperature range down to 263 K. Measurements of a series of certified standards spanning the viscosity and density range of the instrument are required at 293 K, 333 K, and 373 K and at 293 K, 313 K, 333 K, 353 K, and 373 K to adjust the apparatus constants in the instrument's working equations for viscosity and density, respectively. Additional details about the viscodensimeter can be found in Laesecke et al.[16]

With both instruments, sample liquid is injected into the instrument using a disposable syringe. Approximately 3 mL of sample is sufficient to fill both measurement cells (sound speed and density or density and viscosity, depending on the specific instrument). Measurements were made via programmed scans between the maximum and minimum temperature in 5 K decrements. At least five replicate measurement scans were performed for each of the 11 RP-1 samples with a fresh aliquot of sample fluid injected into the instrument prior to the start of each scan. In between RP-1 samples, the measurement cells in both instruments were thoroughly cleaned and dried to ensure that cross-contamination did not occur. Past experience has shown that this is of particular concern with the density and sound speed analyzer; for additional details refer to Fortin et al.[15]

RESULTS AND DISCUSSION

Density. Results of the density measurements made with the density and sound speed analyzer for all 11 RP-1 samples are presented in Table 2. For each sample, the tabulated densities represent the average ($\overline{\rho}$) of five replicate measurement scans. Also included in the table are the associated expanded uncertainty estimates ($U(\overline{\rho})$). The expanded uncertainty is calculated using the expression

$$U(\overline{\rho}) = t_p(\mathrm{df}_\rho)u(\overline{\rho}) \quad (1)$$

where $t_p(\mathrm{df}_\rho)$ is taken from the *t*-distribution for df_ρ degrees of freedom and a p percent level of confidence (typically 95%), and $u(\overline{\rho})$ is the combined standard uncertainty for the averaged density measurements. The corresponding value of $t_p(\mathrm{df}_\rho)$ can be found in table G.2 of the *Guide to the Expression of Uncertainty in Measurement*[17] by interpolation or by truncating df_ρ to the next lower integer. The combined standard uncertainty includes the standard deviation of the average as well as contributions for the uncertainties due to the resolution of the instrument, the instrument's varied response with density range, and the measured temperature. Additional details concerning the uncertainty analysis calculations can be found in Fortin et al.[15] For the density measurements reported in Table 2, the temperature contribution was estimated as 0.03 kg m^{-3} for a ±0.03 K uncertainty in temperature and $t_p(\mathrm{df}_\rho)$ ranged from 2.026 to 2.447. The reported absolute expanded uncertainties (±0.06 to ±0.15 kg m^{-3}) correspond to relative expanded uncertainties of ±0.01% to ±0.02%.

In an effort to more clearly show the variability in density observed among the 11 different RP-1 blends, the averaged densities shown in Table 2 are plotted as a function of temperature in Figure 1. An overall average was calculated for the 11 samples and is also shown in Figure 1 as a solid line. The variability observed in density over the 11 RP-1 samples is relatively constant as a function of temperature, ranging from 1.3% at 278 K to 1.4% at 343 K. A significant contributor to the observed variability is blend 9, which has markedly lower densities than the other blends, 0.5% to 0.6% lower than the next lowest blend (blend 3). Unfortunately, with such complex mixtures it can be difficult, if not impossible, to definitively link observed behavior to what is known about the composition. For example, ignoring the contribution of aromatics

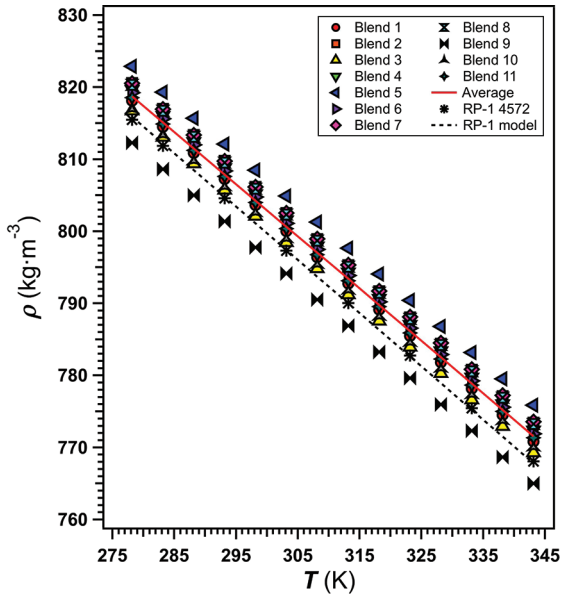

Figure 1. Ambient pressure density measurements for each of the 11 RP-1 samples plotted as a function of temperature. The mean density for all 11 samples is represented as a solid line. Results from earlier measurements of an additional RP-1 sample (RP-1 4572)[18] have been included for comparison. The earlier measurements were made using the same density and sound speed analyzer used in the current work, and the data were used in the development of the current REFPROP[20] surrogate mixture model for RP-1.[19] The RP-1 model predictions are also shown for comparison (dashed line).

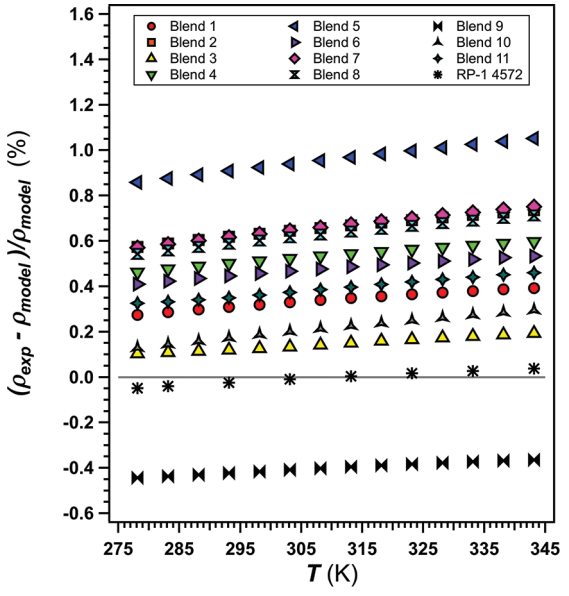

Figure 2. Percent deviations of ambient pressure density measurements from the RP-1 surrogate mixture model[19] for each of the 11 RP-1 samples plotted as a function of temperature. Calculated deviations for earlier measurements of an additional RP-1 sample (RP-1 4572)[18] have been included for comparison.

(which should be relatively small since RP-1 fuel specifications limit aromatics to a maximum of 5% by volume[5]), in general, density should increase with increased intermolecular interactions. For alkanes, the van der Waals forces controlling those interactions will be strongest for molecules whose structure allows for close intermolecular contact. Therefore, one would expect density to increase moving from branched alkanes to linear alkanes to cycloalkanes.

dx.doi.org/10.1021/ef3004009 | Energy Fuels 2012, 26, 4383−4394

Table 3. Speeds of Sound of the 11 RP-1 Samples Measured in the Density and Sound Speed Analyzer at Ambient Pressure[a]

	Blend 1		Blend 2		Blend 3		Blend 4		Blend 5		Blend 6	
T (K)	$\bar{w}$ (m s^{-1})	$U(\bar{w})$ (m s^{-1})	$\bar{w}$ (m s^{-1})	$U(\bar{w})$ (m s^{-1})	$\bar{w}$ (m s^{-1})	$U(\bar{w})$ (m s^{-1})	$\bar{w}$ (m s^{-1})	$U(\bar{w})$ (m s^{-1})	$\bar{w}$ (m s^{-1})	$U(\bar{w})$ (m s^{-1})	$\bar{w}$ (m s^{-1})	$U(\bar{w})$ (m s^{-1})
343.15	1139.7	0.7	1141.6	0.7	1136.5	0.7	1139.3	0.7	1145.1	0.7	1138.2	0.7
338.15	1157.5	0.7	1159.4	0.7	1154.3	0.7	1157.1	0.7	1162.8	0.7	1156.0	0.7
333.15	1175.5	0.7	1177.4	0.7	1172.4	0.7	1175.2	0.7	1180.8	0.7	1174.1	0.7
328.15	1193.7	0.7	1195.6	0.7	1190.6	0.7	1193.4	0.7	1199.0	0.7	1192.3	0.7
323.15	1212.0	0.7	1213.9	0.7	1209.0	0.7	1211.8	0.7	1217.3	0.7	1210.7	0.7
318.15	1230.5	0.7	1232.5	0.7	1227.5	0.7	1230.3	0.7	1235.8	0.7	1229.3	0.7
313.15	1249.2	0.7	1251.2	0.7	1246.3	0.7	1249.1	0.7	1254.5	0.7	1248.2	0.7
308.15	1268.2	0.7	1270.1	0.7	1265.3	0.7	1268.1	0.7	1273.4	0.7	1267.2	0.7
303.15	1287.3	0.7	1289.2	0.7	1284.5	0.7	1287.3	0.7	1292.5	0.7	1286.4	0.7
298.15	1306.6	0.7	1308.5	0.7	1303.8	0.7	1306.7	0.7	1311.8	0.7	1305.8	0.7
293.15	1326.1	0.7	1328.1	0.7	1323.4	0.7	1326.3	0.7	1331.3	0.7	1325.4	0.7
288.15	1345.8	0.7	1347.9	0.7	1343.2	0.7	1346.1	0.7	1351.1	0.7	1345.3	0.7
283.15	1365.8	0.7	1367.9	0.7	1363.2	0.7	1366.2	0.7	1371.1	0.7	1365.3	0.7
278.15	1386.0	0.7	1388.1	0.7	1383.5	0.7	1386.5	0.7	1391.3	0.7	1385.6	0.7

	Blend 7		Blend 8		Blend 9		Blend 10		Blend 11	
T (K)	$\bar{w}$ (m s^{-1})	$U(\bar{w})$ (m s^{-1})	$\bar{w}$ (m s^{-1})	$U(\bar{w})$ (m s^{-1})	$\bar{w}$ (m s^{-1})	$U(\bar{w})$ (m s^{-1})	$\bar{w}$ (m s^{-1})	$U(\bar{w})$ (m s^{-1})	$\bar{w}$ (m s^{-1})	$U(\bar{w})$ (m s^{-1})
343.15	1145.5	0.7	1141.9	0.7	1137.1	0.7	1142.7	0.7	1140.6	0.7
338.15	1163.2	0.7	1159.7	0.7	1154.8	0.7	1160.4	0.7	1158.4	0.7
333.15	1181.1	0.7	1177.7	0.7	1172.8	0.7	1178.4	0.7	1176.3	0.7
328.15	1199.2	0.7	1195.8	0.7	1190.9	0.7	1196.5	0.7	1194.5	0.7
323.15	1217.4	0.7	1214.2	0.7	1209.2	0.7	1214.7	0.7	1212.8	0.7
318.15	1235.9	0.7	1232.7	0.7	1227.7	0.7	1233.2	0.7	1231.3	0.7
313.15	1254.5	0.7	1251.4	0.7	1246.4	0.7	1251.8	0.7	1250.0	0.7
308.15	1273.3	0.7	1270.2	0.7	1265.3	0.7	1270.7	0.7	1268.9	0.7
303.15	1292.4	0.7	1289.3	0.7	1284.4	0.7	1289.7	0.7	1288.0	0.7
298.15	1311.6	0.7	1308.6	0.7	1303.6	0.7	1309.0	0.7	1307.3	0.7
293.15	1331.0	0.7	1328.2	0.7	1323.1	0.7	1328.4	0.7	1326.9	0.7
288.15	1350.7	0.7	1347.9	0.7	1342.7	0.7	1348.1	0.7	1346.6	0.7
283.15	1370.6	0.7	1367.9	0.7	1362.6	0.7	1368.0	0.7	1366.6	0.7
278.15	1390.6	0.7	1388.1	0.7	1382.7	0.7	1388.1	0.7	1386.8	0.7

[a]Ambient pressure during measurements was ~83 kPa.

Interestingly, the reported hydrocarbon classification data shows that blend 9 has the lowest percentage of cycloparaffins (51.7 vol %) and the highest percentage of paraffins (39.0 vol %);[9] however, the relative contributions of straight alkanes vs branched alkanes within the paraffin class does not appear to fit with initial expectations based on structure alone. A detailed examination of the more than 60 compounds identified for each of the 11 samples[9] verifies the observations gleaned from Table 1; blend 9 has the greatest area percentage of straight alkanes relative to branched alkanes at 13.7% and 27.8%, respectively. It is clear from this example that knowledge about the composition of a complex fluid such as RP-1 is not sufficient to draw definitive conclusions about the relative contribution of individual fuel components to the observed trends in density.

Also shown in Figure 1 are previously reported[18] ambient pressure (~83 kPa) density measurements for an older RP-1 sample, designated RP-1 4572. These data have been included because they were measured with the same density and sound speed analyzer used in this work. Furthermore, the RP-1 4572 measurements were utilized during the development of a surrogate mixture model to represent the thermophysical properties of RP-1. Specifically, since RP-1 4572 was considered at the time to be representative of as-delivered RP-1, its composition was used during the selection of the surrogate mixture model constituent fluids, and the thermophysical property measurements of RP-1 4572 were later used to validate the model. That model was developed at NIST, and it has been implemented within the framework of the Reference Fluid Thermodynamic and Transport Properties (REFPROP) database.[19,20] Model predictions for our experimental conditions are shown in Figure 1 as a dashed line. Two observations are immediately apparent when looking at Figure 1. First, as expected, the RP-1 4572 density measurements are in very good agreement with the current RP-1 model. Second, density predictions from the current RP-1 model are lower than all but one (blend 9) of the 11 RP-1 samples measured in this work.

Figure 2 more clearly shows the deviations between the experimental measurements and the current model. Also included in Figure 2 are the calculated deviations for the RP-1 4572 measurements, which range from −0.05% at 278 K to +0.04% at 343 K, well within the reported model uncertainty of 0.4% for density.[19] Deviations for the 11 samples measured in this study also indicate a slight temperature dependence with larger deviations occurring at higher temperatures. Of the 11 blends, blend 3 exhibits the best agreement with the current RP-1 model with deviations of only 0.1% to 0.2%. Blend 5 exhibits the worst agreement with the model with deviations of 0.9% to 1.1%. As was mentioned previously, only blend 9 has densities that are lower than the model with deviations of approximately −0.4%. It is clear from Figures 1 and 2 that the current RP-1 model is able to reproduce the densities of a specific sample (RP-1 4572) very

dx.doi.org/10.1021/ef3004009 | Energy Fuels 2012, 26, 4383−4394

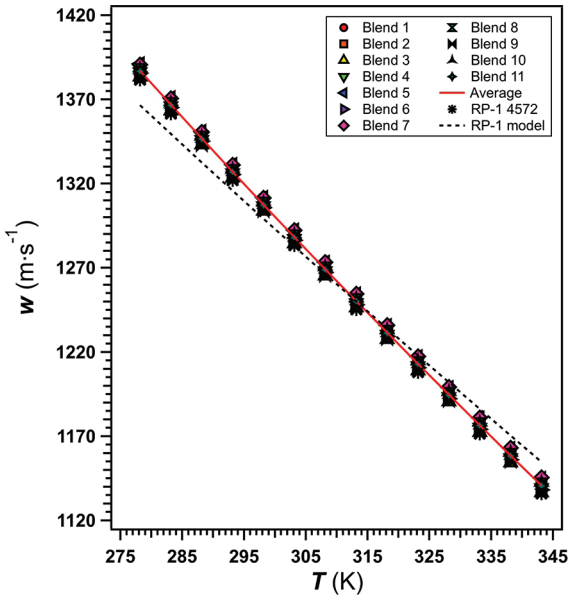

Figure 3. Ambient pressure speed of sound measurements for each of the 11 RP-1 samples plotted as a function of temperature. The mean sound speed for all 11 samples is represented as a solid line. Results from earlier measurements of an additional RP-1 sample (RP-1 4572)[18] have been included for comparison. The earlier measurements were made using the same density and sound speed analyzer used in the current work, and the data were used in the development of the current REFPROP[20] surrogate mixture model for RP-1.[19] The RP-1 model predictions are also shown for comparison (dashed line).

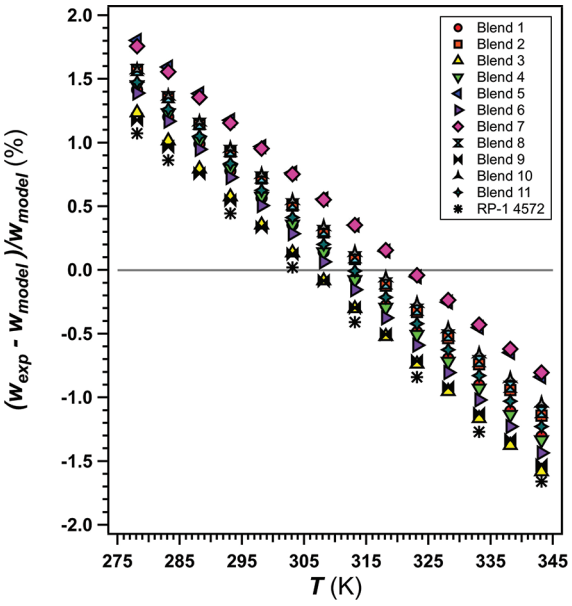

Figure 4. Percent deviations of ambient pressure sound speed measurements from the RP-1 surrogate mixture model[19] for each of the 11 RP-1 samples plotted as a function of temperature. Calculated deviations for earlier measurements of an additional RP-1 sample (RP-1 4572)[18] have been included for comparison.

well; however, it misses the range of densities that might be expected as a result of compositional variability.

Speed of Sound. Results of the sound speed measurements for all 11 RP-1 samples are presented in Table 3. Included in the table are averages ($\bar{w}$) for the five replicate measurement scans performed for each sample and the associated expanded uncertainty estimates ($U(\bar{w})$). Expanded uncertainties for sound speed measurements were calculated using a method analogous to that previously described for density measurements; additional details can be found in Fortin et al.[15] For the sound speed measurements reported in Table 3, the temperature contribution was estimated as 0.13 m s^{-1} for a ±0.03 K uncertainty in temperature and $t_p(df_w)$ ranged from 2.011 to 2.014. The reported absolute expanded uncertainties (±0.7 m s^{-1}) correspond to relative expanded uncertainties of ±0.06%.

The averaged sound speeds shown in Table 3 are plotted as a function of temperature in Figure 3. An overall average was calculated for the 11 samples, and it is also shown in Figure 3 as a solid line. Similar to density, the variability observed in speed of sound over the 11 RP-1 samples is relatively independent of temperature, ranging from 0.6% at 278 K to 0.8% at 343 K. However, these percentages are almost a factor of 2 smaller than what was observed for density.

Also shown in Figure 3 are previously reported[18] ambient pressure (~83 kPa) sound speed measurements for RP-1 4572, as well as RP-1 model[19] predictions calculated for our experimental conditions (dashed line). It is clear from looking at Figure 3 that there is a difference between the experimental measurements and the current RP-1 model in the slope of the observed temperature dependence in speed of sound. This is true even when the model is compared to the RP-1 4572 sound speed results, which are similar to the lower range of sound speeds observed in this work, particularly blends 3 and 9.

Figure 4 shows the calculated deviations between the experimental measurements and the current model. Percent deviations were calculated for the 11 RP-1 samples, as well as for RP-1 4572. In contrast to the slight temperature dependence observed with density, Figure 4 shows a strong temperature dependence in calculated deviations, which change sign from positive to negative as temperature is increased. Deviations for RP-1 4572 range from +1.1% at 278 K to −1.7% at 343 K. Deviations for the 11 blends range from +1.2% to +1.8% at 278 K to −1.6% to −0.8% at 343 K. In contrast to density, all of the observed deviations are within the reported model uncertainty of 2% for speed of sound.[19] However, whereas the model is able to reproduce the measured densities of RP-1 4572 within reported experimental uncertainties, this is not the case for the measured speeds of sound of RP-1 4572. This can be largely attributed to the scarcity of experimental data for the pure components that make up the surrogate mixture, particularly since data availability tends to be worse for sound speeds compared to densities.

Adiabatic Compressibility. Using the measured densities and speeds of sound presented in Tables 2 and 3, adiabatic compressibilities (κ_s) were calculated via the thermodynamic relationship

$$\kappa_s = \frac{1}{\rho w^2} \tag{2}$$

where ρ is the density, w is the speed of sound, and the subscript s indicates "at constant entropy". The results of these calculations for all 11 RP-1 samples are presented in Table 4. Included in the table are the averages ($\bar{\kappa}_s$) of five replicate measurement scans of density and speed of sound and the associated expanded uncertainty estimates ($U(\bar{\kappa}_s)$). Since the adiabatic compressibility is derived from two measured quantities, the expanded relative uncertainties associated with density and speed of sound were combined in quadrature to determine the expanded uncertainties reported in Table 4. The reported absolute expanded uncertainties (±0.3 TPa^{-1} to ±0.7 TPa^{-1}) correspond to relative expanded uncertainties of ±0.05% to ±0.07%.

dx.doi.org/10.1021/ef3004009 | Energy Fuels 2012, 26, 4383−4394

Table 4. Calculated Adiabatic Compressibilities for the 11 RP-1 Samples at Ambient Pressure[a]

	Blend 1		Blend 2		Blend 3		Blend 4		Blend 5		Blend 6	
T (K)	$\bar{\kappa}_s$ (TPa^{-1})	$U(\bar{\kappa}_s)$ (TPa^{-1})	$\bar{\kappa}_s$ (TPa^{-1})	$U(\bar{\kappa}_s)$ (TPa^{-1})	$\bar{\kappa}_s$ (TPa^{-1})	$U(\bar{\kappa}_s)$ (TPa^{-1})	$\bar{\kappa}_s$ (TPa^{-1})	$U(\bar{\kappa}_s)$ (TPa^{-1})	$\bar{\kappa}_s$ (TPa^{-1})	$U(\bar{\kappa}_s)$ (TPa^{-1})	$\bar{\kappa}_s$ (TPa^{-1})	$U(\bar{\kappa}_s)$ (TPa^{-1})
343.15	998.8	0.6	992.1	0.6	1006.4	0.7	997.4	0.6	983.0	0.6	1000.0	0.6
338.15	963.7	0.6	957.3	0.6	970.9	0.6	962.4	0.6	948.7	0.6	964.8	0.6
333.15	930.0	0.6	923.9	0.6	936.8	0.6	928.7	0.6	915.7	0.6	930.9	0.6
328.15	897.7	0.6	891.9	0.6	904.1	0.6	896.3	0.6	884.1	0.6	898.5	0.6
323.15	866.7	0.5	861.1	0.5	872.8	0.5	865.3	0.5	853.8	0.5	867.3	0.5
318.15	836.9	0.5	831.6	0.5	842.6	0.5	835.5	0.5	824.6	0.5	837.3	0.5
313.15	808.3	0.5	803.2	0.5	813.7	0.5	806.8	0.5	796.6	0.5	808.6	0.5
308.15	780.8	0.5	775.9	0.5	785.9	0.5	779.3	0.5	769.6	0.4	780.9	0.5
303.15	754.3	0.4	749.7	0.4	759.1	0.4	752.8	0.4	743.7	0.4	754.3	0.4
298.15	728.9	0.4	724.4	0.4	733.4	0.4	727.3	0.4	718.8	0.4	728.8	0.4
293.15	704.4	0.4	700.1	0.4	708.6	0.4	702.8	0.4	694.7	0.4	704.2	0.4
288.15	680.9	0.4	676.7	0.4	684.8	0.4	679.3	0.4	671.6	0.4	680.5	0.4
283.15	658.2	0.4	654.2	0.4	661.8	0.4	656.5	0.4	649.3	0.4	657.7	0.4
278.15	636.3	0.3	632.5	0.3	639.7	0.4	634.7	0.3	627.8	0.3	635.8	0.3

	Blend 7		Blend 8		Blend 9		Blend 10		Blend 11	
T (K)	$\bar{\kappa}_s$ (TPa^{-1})	$U(\bar{\kappa}_s)$ (TPa^{-1})	$\bar{\kappa}_s$ (TPa^{-1})	$U(\bar{\kappa}_s)$ (TPa^{-1})	$\bar{\kappa}_s$ (TPa^{-1})	$U(\bar{\kappa}_s)$ (TPa^{-1})	$\bar{\kappa}_s$ (TPa^{-1})	$U(\bar{\kappa}_s)$ (TPa^{-1})	$\bar{\kappa}_s$ (TPa^{-1})	$U(\bar{\kappa}_s)$ (TPa^{-1})
343.15	985.2	0.6	991.8	0.6	1011.0	0.7	994.5	0.6	996.5	0.6
338.15	951.0	0.6	957.0	0.6	975.5	0.6	959.8	0.6	961.6	0.6
333.15	918.0	0.6	923.7	0.6	941.3	0.6	926.4	0.6	928.1	0.6
328.15	886.5	0.5	891.7	0.5	908.6	0.6	894.5	0.6	895.9	0.6
323.15	856.1	0.5	861.0	0.5	877.2	0.5	863.8	0.5	865.1	0.5
318.15	826.9	0.5	831.5	0.5	847.0	0.5	834.3	0.5	835.4	0.5
313.15	798.9	0.5	803.2	0.5	818.0	0.5	805.9	0.5	806.9	0.5
308.15	772.0	0.5	776.0	0.5	790.1	0.5	778.6	0.5	779.5	0.5
303.15	746.0	0.4	749.8	0.4	763.4	0.4	752.4	0.4	753.1	0.4
298.15	721.1	0.4	724.5	0.4	737.6	0.4	727.2	0.4	727.7	0.4
293.15	697.1	0.4	700.3	0.4	712.9	0.4	702.9	0.4	703.3	0.4
288.15	673.9	0.4	676.9	0.4	689.0	0.4	679.5	0.4	679.7	0.4
283.15	651.6	0.4	654.4	0.4	666.0	0.4	657.0	0.4	657.1	0.4
278.15	630.2	0.3	632.7	0.3	643.9	0.4	635.3	0.3	635.2	0.4

[a]Ambient pressure during measurements was ~83 kPa.

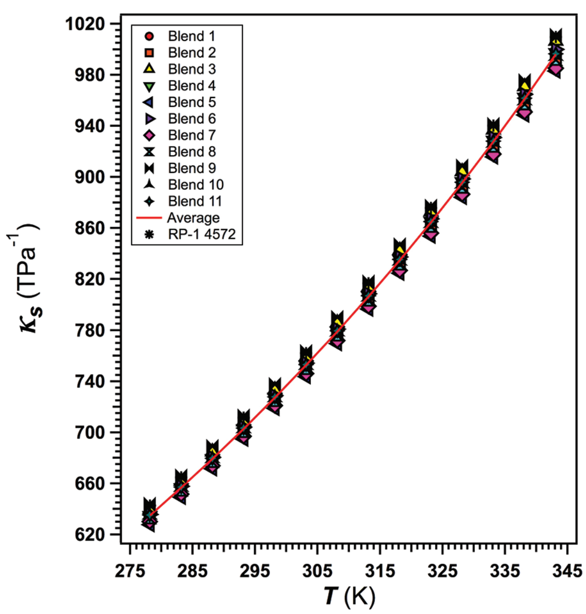

Figure 5. Calculated ambient pressure adiabatic compressibilities for each of the 11 RP-1 samples plotted as a function of temperature. The mean adiabatic compressibility for all 11 samples is represented as a solid line. Results from earlier measurements of an additional RP-1 sample (RP-1 4572)[18] have been included for comparison. The earlier measurements were made using the same density and sound speed analyzer used in the current work.

The averaged adiabatic compressibilities shown in Table 4 are plotted as a function of temperature in Figure 5. An overall average was calculated for the 11 samples, and it is also shown in Figure 5 as a solid line. The variability observed in adiabatic compressibility over the 11 RP-1 samples is larger than that observed for either density or speed of sound, ranging from 2.5% at 278 K to 2.8% at 343 K. Previously reported[18] adiabatic compressibilities for RP-1 4572 are also included in Figure 5 for comparison. With density (Figure 1), RP-1 4572 has values between those observed for blends 3 and 9 and is most similar to blend 3 with values that are approximately 0.2% lower than blend 3. With sound speed (Figure 3), RP-1 4572 has values that are lower than all 11 blends and is most similar to blend 9 at 278 K and most similar to blend 3 at 343 K with values that are approximately 0.1% lower for both blends. With adiabatic compressibilities (Figure 5), RP-1 4572 again has values that lie between blends 3 and 9 and is most similar to blend 9. Adiabatic compressibilities for RP-1 4572 range from 0.2% lower than blend 9 at 278 K to 0.1% lower at 343 K.

Viscosity. Results of the dynamic viscosity measurements made with the viscodensimeter for all 11 RP-1 samples are presented in Table 5. For each sample, the tabulated dynamic viscosities represent the average ($\bar{\eta}$) of at least five replicate measurement scans. Also included in the table are the associated expanded uncertainty estimates ($U(\bar{\eta})$). Expanded uncertainties for dynamic viscosity measurements were calculated using a method analogous to that previously described for density and speed of sound measurements; additional details can be found in Fortin et al.[15] and Laesecke et al.[16] For the dynamic viscosity

Table 5. Dynamic Viscosities of the 11 RP-1 Samples Measured in the Viscodensimeter at Ambient Pressure[a]

	Blend 1		Blend 2		Blend 3		Blend 4		Blend 5		Blend 6	
T (K)	$\overline{\eta}$ (mPa s)	$U(\overline{\eta})$ (mPa s)	$\overline{\eta}$ (mPa s)	$U(\overline{\eta})$ (mPa s)	$\overline{\eta}$ (mPa s)	$U(\overline{\eta})$ (mPa s)	$\overline{\eta}$ (mPa s)	$U(\overline{\eta})$ (mPa s)	$\overline{\eta}$ (mPa s)	$U(\overline{\eta})$ (mPa s)	$\overline{\eta}$ (mPa s)	$U(\overline{\eta})$ (mPa s)
373.15	0.6001	0.0083	0.6278	0.0067	0.6074	0.0074	0.6033	0.0062	0.6343	0.0066	0.6005	0.0062
368.15	0.6332	0.0085	0.6631	0.0067	0.6409	0.0074	0.6363	0.0062	0.6697	0.0067	0.6332	0.0062
363.15	0.6694	0.0088	0.7016	0.0067	0.6776	0.0077	0.6725	0.0062	0.7085	0.0067	0.6692	0.0062
358.15	0.7084	0.0091	0.7434	0.0068	0.7177	0.0082	0.7122	0.0062	0.7511	0.0068	0.7085	0.0062
353.15	0.7511	0.0093	0.7891	0.0068	0.7611	0.0087	0.7556	0.0063	0.7979	0.0068	0.7515	0.0063
348.15	0.7982	0.0096	0.8395	0.0069	0.8088	0.0092	0.8029	0.0063	0.8489	0.0068	0.7984	0.0063
343.15	0.8502	0.0100	0.8952	0.0070	0.8616	0.0100	0.8552	0.0063	0.9053	0.0069	0.8502	0.0064
338.15	0.9078	0.0104	0.9571	0.0071	0.9203	0.0106	0.9131	0.0064	0.9681	0.0070	0.9076	0.0065
333.15	0.9718	0.0109	1.026	0.007	0.9854	0.0116	0.9775	0.0065	1.038	0.007	0.9714	0.0067
328.15	1.043	0.012	1.103	0.007	1.058	0.013	1.049	0.007	1.116	0.007	1.043	0.007
323.15	1.124	0.012	1.190	0.008	1.140	0.014	1.130	0.007	1.204	0.007	1.123	0.007
318.15	1.214	0.013	1.288	0.008	1.232	0.015	1.221	0.007	1.304	0.008	1.213	0.007
313.15	1.316	0.015	1.400	0.008	1.337	0.017	1.324	0.007	1.417	0.008	1.315	0.007
308.15	1.433	0.016	1.528	0.008	1.457	0.019	1.442	0.007	1.547	0.009	1.431	0.008
303.15	1.567	0.017	1.675	0.009	1.594	0.021	1.577	0.008	1.697	0.009	1.565	0.008
298.15	1.722	0.019	1.846	0.009	1.753	0.023	1.733	0.008	1.870	0.010	1.719	0.009
293.15	1.903	0.020	2.046	0.009	1.938	0.027	1.915	0.009	2.072	0.012	1.898	0.010
288.15	2.115	0.022	2.282	0.010	2.156	0.030	2.128	0.010	2.312	0.013	2.109	0.012
283.15	2.366	0.026	2.563	0.010	2.415	0.034	2.381	0.012	2.596	0.016	2.358	0.014
278.15	2.667	0.029	2.901	0.011	2.726	0.039	2.683	0.014	2.939	0.020	2.657	0.016
273.15	3.032	0.033	3.313	0.011	3.102	0.045	3.050	0.017	3.357	0.024	3.018	0.020
268.15	3.477	0.038	3.820	0.011	3.563	0.054	3.499	0.021	3.872	0.031	3.460	0.026
263.15	4.029	0.044	4.453	0.012	4.136	0.065	4.056	0.027	4.515	0.039	4.007	0.033

	Blend 7		Blend 8		Blend 9		Blend 10		Blend 11	
T (K)	$\overline{\eta}$ (mPa s)	$U(\overline{\eta})$ (mPa s)	$\overline{\eta}$ (mPa s)	$U(\overline{\eta})$ (mPa s)	$\overline{\eta}$ (mPa s)	$U(\overline{\eta})$ (mPa s)	$\overline{\eta}$ (mPa s)	$U(\overline{\eta})$ (mPa s)	$\overline{\eta}$ (mPa s)	$U(\overline{\eta})$ (mPa s)
373.15	0.6379	0.0069	0.6300	0.0067	0.6062	0.0072	0.6401	0.0071	0.6250	0.0067
368.15	0.6735	0.0069	0.6651	0.0068	0.6395	0.0074	0.6760	0.0072	0.6599	0.0068
363.15	0.7127	0.0070	0.7038	0.0068	0.6759	0.0077	0.7156	0.0073	0.6979	0.0069
358.15	0.7556	0.0070	0.7459	0.0069	0.7157	0.0080	0.7589	0.0075	0.7397	0.0070
353.15	0.8027	0.0071	0.7921	0.0070	0.7595	0.0084	0.8065	0.0077	0.7856	0.0072
348.15	0.8541	0.0072	0.8425	0.0071	0.8072	0.0087	0.8585	0.0078	0.8359	0.0073
343.15	0.9110	0.0074	0.8985	0.0073	0.8599	0.0092	0.9159	0.0081	0.8910	0.0073
338.15	0.9742	0.0076	0.9606	0.0075	0.9183	0.0097	0.9799	0.0085	0.9525	0.0075
333.15	1.045	0.008	1.030	0.008	0.9833	0.0104	1.051	0.009	1.021	0.008
328.15	1.124	0.008	1.107	0.008	1.056	0.011	1.131	0.009	1.098	0.008
323.15	1.213	0.008	1.194	0.008	1.138	0.012	1.221	0.010	1.184	0.009
318.15	1.313	0.009	1.293	0.009	1.230	0.014	1.324	0.011	1.282	0.009
313.15	1.428	0.010	1.405	0.010	1.334	0.015	1.440	0.012	1.392	0.010
308.15	1.559	0.010	1.533	0.011	1.453	0.017	1.573	0.013	1.519	0.011
303.15	1.710	0.012	1.681	0.012	1.590	0.020	1.727	0.015	1.665	0.012
298.15	1.886	0.013	1.852	0.013	1.748	0.022	1.905	0.018	1.834	0.014
293.15	2.092	0.015	2.052	0.015	1.933	0.027	2.115	0.021	2.032	0.016
288.15	2.335	0.017	2.288	0.018	2.151	0.031	2.362	0.024	2.266	0.018
283.15	2.625	0.021	2.569	0.022	2.409	0.036	2.658	0.030	2.543	0.022
278.15	2.974	0.024	2.908	0.025	2.718	0.043	3.014	0.036	2.878	0.028
273.15	3.401	0.031	3.320	0.033	3.094	0.051	3.450	0.043	3.284	0.034
268.15	3.928	0.037	3.828	0.040	3.555	0.062	3.989	0.052	3.785	0.041
263.15	4.586	0.046	4.462	0.051	4.127	0.076	4.663	0.065	4.410	0.051

[a]Ambient pressure during measurements was ~83 kPa.

measurements reported in Table 5, the temperature contribution was estimated as 0.0009 mPa s for a ±0.03 K uncertainty in temperature and $t_p(df_\eta)$ ranged from 1.995 to 2.776. The reported absolute expanded uncertainties (±0.006 mPa s to ±0.076 mPa s) correspond to relative expanded uncertainties of ±0.3% to ±1.8%.

The averaged dynamic viscosities shown in Table 5 are plotted as a function of temperature in Figure 6. An overall average was calculated for the 11 samples and it is also shown in Figure 6 as a solid line. The variability observed in dynamic viscosity over the 11 RP-1 samples is significantly larger than that observed for either density or speed of sound and, unlike the previous properties, it changes considerably with temperature. The overall variability for the 11 samples ranges from 14.1% at 263 K to 6.2% at 373 K. Furthermore, the observed dynamic viscosities are separated into

dx.doi.org/10.1021/ef3004009 | Energy Fuels 2012, 26, 4383−4394

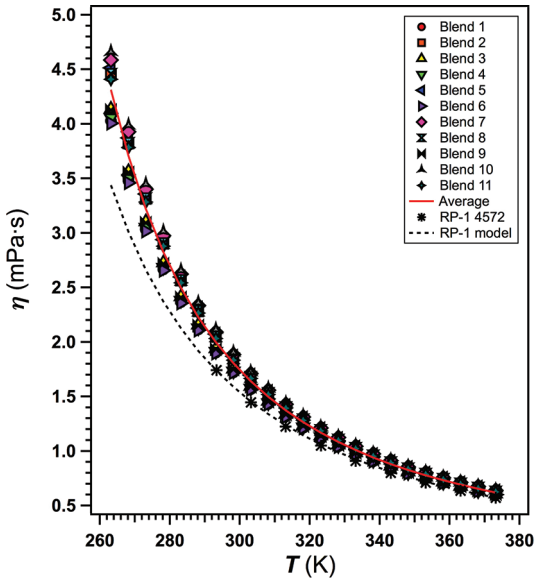

Figure 6. Ambient pressure dynamic viscosity measurements for each of the 11 RP-1 samples plotted as a function of temperature. The mean dynamic viscosity for all 11 samples is represented as a solid line. Previously reported values for an additional RP-1 sample (RP-1 4572)[18] and current RP-1 surrogate mixture model[19] predictions (dashed line) are also shown for comparison.

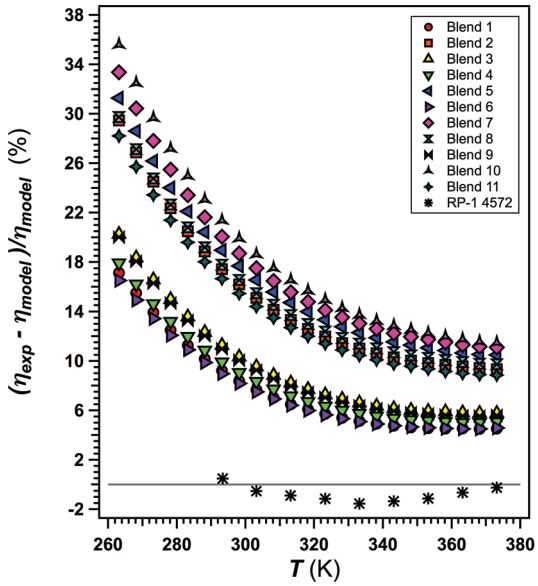

Figure 7. Percent deviations of ambient pressure dynamic viscosity measurements from the RP-1 surrogate mixture model[19] for each of the 11 RP-1 samples plotted as a function of temperature. Calculated deviations for an additional RP- 1 sample (RP-1 4572)[18] have been included for comparison.

two distinct clusters, each with smaller but still significant blend-to-blend variability. The cluster with the higher overall dynamic viscosities consists of blends 2, 5, 7, 8, 10, and 11. The variability for this first cluster ranges from 5.4% at 263 K to 2.4% at 373 K. The cluster with the lower overall dynamic viscosities includes blends 1, 3, 4, 6, and 9. The variability for this second cluster ranges from 3.1% at 263 K to 1.2% at 373 K.

Also shown in Figure 6 are previously reported[18] ambient pressure (~83 kPa) dynamic viscosity values for RP-1 4572, as well as RP-1 model predictions calculated for our experimental conditions (dashed line). As was previously discussed in the Materials and Methods section, in this work dynamic viscosity was measured directly with a viscodensimeter. In contrast, Outcalt et al.[18] used an automated open gravitational flow viscometer to measure kinematic viscosity and then combined those measurements with their density measurements to calculate dynamic viscosity. The relationship between dynamic and kinematic viscosity is discussed further below. Note that the lower temperature limit for the kinematic viscosity measurements of Outcalt et al.[18] is 293 K. Two observations can be made when looking at Figure 6. First, the RP-1 4572 dynamic viscosity values are in very good agreement with the current RP-1 model. This is not surprising since the experimental data of Outcalt et al.[18] were utilized during the development and validation of the RP-1 model.[19] Second, dynamic viscosity predictions from the current RP-1 model are lower than all of the 11 RP-1 samples measured in this work, significantly so at colder temperatures.

The calculated deviations between the experimental measurements and the current model are shown in Figure 7. The figure includes percent deviations for all 11 RP-1 samples, as well as for RP-1 4572. The close agreement between RP-1 4572 and the RP-1 model is readily apparent in Figure 7. The experimental dynamic viscosity values for RP-1 4572 are, overall, slightly lower than the model. The single exception occurs at 293 K where RP-1 4572 is 0.5% higher than the model. Otherwise, the best agreement between RP-1 4572 and the model is observed at 373K (−0.2%) while the worst agreement is observed at 333 K (−1.6%). At all temperatures, the agreement between RP-1 4572 and the model are essentially within the estimated expanded uncertainties of the experimental data (1.5%[18]), as well as within the reported model uncertainty of 2% for viscosity.[19] This is in direct contrast to what is observed with the 11 RP-1 samples measured in this work; deviations exceed estimated expanded uncertainties of the experimental data by more than a factor of 2 in the best case (+4.5% for blend 1 at 373 K) and by more than a factor of 25 in the worst case (+35.6% for blend 10 at 263 K). Overall, the current model is not able to represent the range of dynamic viscosities that may result from variations in composition, nor does it represent the observed temperature dependence, particularly at lower temperatures.

Also of note is that the two clusters alluded to earlier are more clearly discernible in Figure 7. For the higher viscosity cluster, which is made up of blends 2, 5, 7, 8, 10, and 11, the observed deviations range from +28.2% to +35.6% at 263 K and from +8.9% to +11.5% at 373 K. The lower viscosity cluster, which is made up of blends 1, 3, 4, 6, and 9, exhibits deviations ranging from +16.5% to +20.3% at 263 K and from +4.5% to +5.8% at 373 K. Unfortunately, as was mentioned earlier, with such complex mixtures it can be difficult to definitively link observed behavior to what is known about the composition. This is particularly true when trying to explain the appearance of the two clusters in Figures 6 and 7; no clear trend could be found among the reported hydrocarbon classification data or among the reported component retention times that could explain the separation. For example, while the lower viscosity cluster includes the two blends with the highest concentrations of straight alkanes relative to branched alkanes (i.e., blends 1 and 9), it also includes the two blends with the lowest concentrations (i.e., blends 4 and 6).[9] Similarly, the higher viscosity cluster includes the blend with the highest concentration of light components (i.e., components with retention times of less than 5 min), blend 11 with 1.6%, as well as the blend with the lowest concentration, blend 5 with 0.6%.[9] However, a trend can be

dx.doi.org/10.1021/ef3004009 | Energy Fuels 2012, 26, 4383−4394

Table 6. Kinematic Viscosities of the 11 RP-1 Samples Measured in the Viscodensimeter at Ambient Pressure[a]

	Blend 1		Blend 2		Blend 3		Blend 4		Blend 5		Blend 6	
T (K)	$\overline{\nu}$ (mm^2 s^{-1})	$U(\overline{\nu})$ (mm^2 s^{-1})	$\overline{\nu}$ (mm^2 s^{-1})	$U(\overline{\nu})$ (mm^2 s^{-1})	$\overline{\nu}$ (mm^2 s^{-1})	$U(\overline{\nu})$ (mm^2 s^{-1})	$\overline{\nu}$ (mm^2 s^{-1})	$U(\overline{\nu})$ (mm^2 s^{-1})	$\overline{\nu}$ (mm^2 s^{-1})	$U(\overline{\nu})$ (mm^2 s^{-1})	$\overline{\nu}$ (mm^2 s^{-1})	$U(\overline{\nu})$ (mm^2 s^{-1})
373.15	0.8024	0.0111	0.8351	0.0090	0.8114	0.0099	0.8050	0.0082	0.8420	0.0088	0.8016	0.0083
368.15	0.8424	0.0114	0.8777	0.0089	0.8519	0.0099	0.8449	0.0082	0.8845	0.0088	0.8411	0.0082
363.15	0.8861	0.0117	0.9241	0.0089	0.8962	0.0102	0.8886	0.0082	0.9313	0.0089	0.8845	0.0082
358.15	0.9331	0.0120	0.9744	0.0089	0.9445	0.0108	0.9364	0.0082	0.9825	0.0089	0.9319	0.0082
353.15	0.9845	0.0122	1.029	0.009	0.9968	0.0114	0.9886	0.0082	1.039	0.009	0.9836	0.0083
348.15	1.041	0.013	1.090	0.009	1.054	0.012	1.045	0.008	1.100	0.009	1.040	0.008
343.15	1.104	0.013	1.157	0.009	1.118	0.013	1.108	0.008	1.167	0.009	1.102	0.008
338.15	1.173	0.013	1.231	0.009	1.188	0.014	1.178	0.008	1.242	0.009	1.171	0.008
333.15	1.250	0.014	1.313	0.009	1.266	0.015	1.255	0.008	1.326	0.009	1.247	0.009
328.15	1.335	0.015	1.406	0.009	1.353	0.016	1.341	0.008	1.419	0.009	1.332	0.009
323.15	1.431	0.015	1.509	0.010	1.451	0.018	1.437	0.009	1.524	0.010	1.428	0.009
318.15	1.539	0.016	1.626	0.010	1.562	0.019	1.546	0.009	1.643	0.010	1.535	0.009
313.15	1.661	0.019	1.760	0.010	1.687	0.021	1.668	0.009	1.778	0.010	1.657	0.009
308.15	1.800	0.020	1.912	0.011	1.829	0.024	1.808	0.009	1.931	0.011	1.796	0.010
303.15	1.960	0.021	2.086	0.011	1.993	0.026	1.969	0.010	2.108	0.012	1.954	0.010
298.15	2.144	0.023	2.289	0.011	2.181	0.028	2.154	0.011	2.313	0.013	2.137	0.011
293.15	2.358	0.025	2.525	0.012	2.401	0.033	2.369	0.012	2.553	0.014	2.350	0.013
288.15	2.610	0.027	2.804	0.012	2.659	0.038	2.621	0.013	2.835	0.017	2.599	0.014
283.15	2.907	0.032	3.135	0.013	2.965	0.042	2.920	0.015	3.170	0.020	2.893	0.017
278.15	3.262	0.036	3.533	0.013	3.331	0.048	3.276	0.017	3.573	0.024	3.245	0.020
273.15	3.692	0.040	4.018	0.014	3.775	0.055	3.707	0.020	4.063	0.029	3.670	0.025
268.15	4.216	0.046	4.613	0.014	4.317	0.065	4.235	0.025	4.666	0.037	4.188	0.032
263.15	4.863	0.054	5.354	0.015	4.989	0.079	4.887	0.033	5.417	0.047	4.830	0.040

	Blend 7		Blend 8		Blend 9		Blend 10		Blend 11	
T (K)	$\overline{\nu}$ (mm^2 s^{-1})	$U(\overline{\nu})$ (mm^2 s^{-1})	$\overline{\nu}$ (mm^2 s^{-1})	$U(\overline{\nu})$ (mm^2 s^{-1})	$\overline{\nu}$ (mm^2 s^{-1})	$U(\overline{\nu})$ (mm^2 s^{-1})	$\overline{\nu}$ (mm^2 s^{-1})	$U(\overline{\nu})$ (mm^2 s^{-1})	$\overline{\nu}$ (mm^2 s^{-1})	$U(\overline{\nu})$ (mm^2 s^{-1})
373.15	0.8494	0.0091	0.8383	0.0090	0.8152	0.0097	0.8542	0.0095	0.8343	0.0090
368.15	0.8924	0.0092	0.8806	0.0090	0.8556	0.0099	0.8977	0.0096	0.8764	0.0091
363.15	0.9397	0.0092	0.9272	0.0090	0.8998	0.0103	0.9456	0.0097	0.9223	0.0091
358.15	0.9915	0.0093	0.9780	0.0091	0.9481	0.0106	0.9979	0.0098	0.9728	0.0092
353.15	1.048	0.009	1.034	0.009	1.001	0.011	1.055	0.010	1.028	0.009
348.15	1.110	0.009	1.094	0.009	1.059	0.011	1.118	0.010	1.089	0.010
343.15	1.178	0.010	1.161	0.009	1.123	0.012	1.187	0.011	1.155	0.009
338.15	1.254	0.010	1.236	0.010	1.193	0.013	1.264	0.011	1.229	0.010
333.15	1.339	0.010	1.319	0.010	1.272	0.014	1.350	0.012	1.311	0.010
328.15	1.433	0.010	1.411	0.010	1.359	0.014	1.446	0.012	1.403	0.010
323.15	1.539	0.011	1.515	0.011	1.457	0.016	1.554	0.013	1.506	0.011
318.15	1.660	0.011	1.633	0.011	1.568	0.017	1.676	0.014	1.623	0.012
313.15	1.796	0.012	1.766	0.012	1.693	0.020	1.815	0.015	1.755	0.013
308.15	1.952	0.013	1.918	0.013	1.836	0.021	1.974	0.017	1.907	0.014
303.15	2.132	0.014	2.094	0.015	2.000	0.025	2.157	0.019	2.080	0.015
298.15	2.341	0.016	2.297	0.017	2.189	0.028	2.369	0.022	2.282	0.017
293.15	2.584	0.018	2.533	0.019	2.410	0.034	2.618	0.026	2.516	0.020
288.15	2.872	0.021	2.812	0.022	2.669	0.039	2.912	0.030	2.793	0.022
283.15	3.214	0.025	3.144	0.027	2.975	0.045	3.262	0.037	3.121	0.027
278.15	3.627	0.030	3.543	0.031	3.343	0.053	3.683	0.044	3.516	0.034
273.15	4.129	0.037	4.027	0.040	3.788	0.062	4.197	0.052	3.995	0.041
268.15	4.747	0.045	4.623	0.049	4.333	0.075	4.832	0.063	4.585	0.049
263.15	5.520	0.056	5.365	0.061	5.009	0.093	5.624	0.079	5.318	0.062

[a]Ambient pressure during measurements was ~83 kPa.

found among the distillation curve data reported by Lovestead et al.;[9] all of the blends that make up the lower viscosity cluster have the lowest reported temperatures for the 50%, 55%, and 60% distillate volume fractions.

In addition to dynamic viscosities, the viscodensimeter automatically calculates and records kinematic viscosities (ν) via the thermodynamic relationship

$$\nu = \frac{\eta}{\rho} \qquad (3)$$

where η and ρ are the measured dynamic viscosity and density at each temperature. Kinematic viscosity results for all 11 RP-1 samples are presented in Table 6. As with the other properties, included in the table are the averages ($\overline{\nu}$) of at least five replicate measurement

dx.doi.org/10.1021/ef3004009 | Energy Fuels 2012, 26, 4383−4394

scans and the associated expanded uncertainty estimates ($U(\overline{\nu})$). As was the case with the adiabatic compressibilities, because the kinematic viscosity is derived from two measured quantities, the expanded relative uncertainties associated with dynamic viscosity and density were combined in quadrature to determine the expanded uncertainties reported in Table 6. The reported absolute expanded uncertainties (± 0.008 mm^2 s^{-1} to ± 0.093 mm^2 s^{-1}) correspond to relative expanded uncertainties of $\pm 0.3\%$ to $\pm 1.9\%$.

The averaged kinematic viscosities shown in Table 6 are plotted as a function of temperature in Figure 8. The solid line

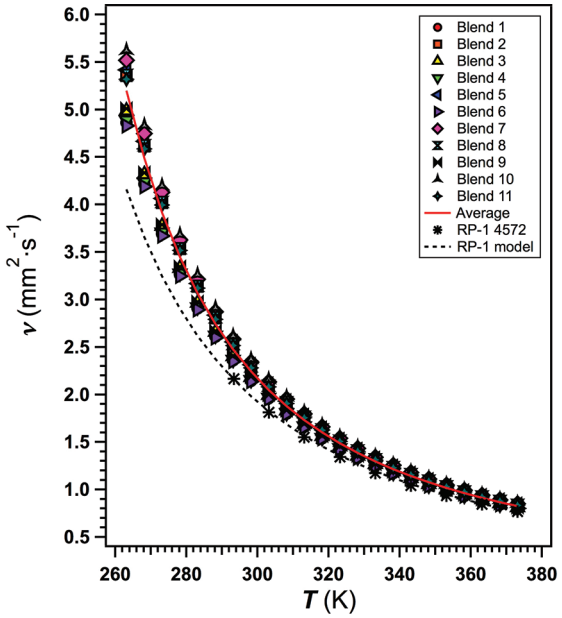

Figure 8. Ambient pressure kinematic viscosity measurements for each of the 11 RP-1 samples plotted as a function of temperature. The mean kinematic viscosity for all 11 samples is represented as a solid line. Results from earlier measurements of an additional RP-1 sample (RP-1 4572)[18] have been included for comparison. The earlier measurements were made using an apparatus different from that used in the current work, and the data were used in the development of the current REFPROP[20] surrogate mixture model for RP-1.[19] The RP-1 model predictions are also shown for comparison (dashed line).

also shown in Figure 8 represents the overall average that was calculated for the 11 samples. The variability in kinematic viscosity is similar to what was observed with dynamic viscosity (Figure 6). This is of course expected since our kinematic viscosity values are derived from the measured dynamic viscosities. The overall variability for the 11 samples ranges from 14.1% at 263 K to 6.2% at 373 K.

Previously reported[18] ambient pressure (~83 kPa) kinematic viscosity measurements for RP-1 4572, as well as RP-1 model predictions calculated for our experimental conditions (dashed line), are also shown in Figure 8 for comparison. As was discussed above, whereas our kinematic viscosities are calculated quantities, the kinematic viscosities reported by Outcalt et al.[18] were measured directly using an instrument different from either of the two that were utilized in this work. As was the case with the dynamic viscosities, the RP-1 4572 kinematic viscosity measurements are in very good agreement with the current RP-1 model and model predictions are lower than all of the 11 RP-1 samples measured in this work.

Figure 9 shows the calculated deviations between the experimental measurements and the current model. Percent deviations

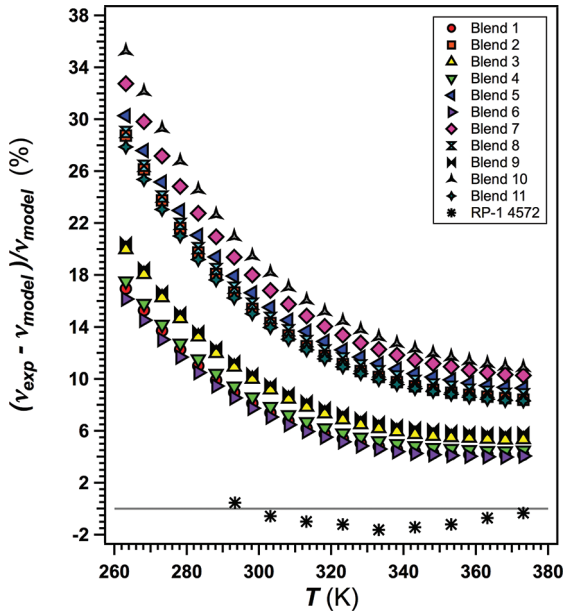

Figure 9. Percent deviations of ambient pressure kinematic viscosity measurements from the RP-1 surrogate mixture model[19] for each of the 11 RP-1 samples plotted as a function of temperature. Calculated deviations for earlier measurements of an additional RP-1 sample (RP-1 4572)[18] have been included for comparison.

were calculated for the 11 RP-1 samples, as well as for RP-1 4572. The close agreement between RP-1 4572 and the RP-1 model is readily apparent in Figure 9 with the best agreement occurring at 373 K (−0.3%) and the worst agreement occurring at 333 K (−1.6%). In contrast, the worst agreement for the 11 RP-1 samples measured in this work occurs at 263 K (blend 10 with +35.2%) and the best agreement occurs at 373 K (blend 6 with +4.1%). Also observed in Figure 9 are the same two clusters, made up of the same blends, that were observed with the dynamic viscosities (Figure 7). For kinematic viscosity, the higher viscosity cluster exhibits deviations ranging from +27.9% to +35.2% at 263 K and from +8.3% to +10.9% at 373 K. For the lower viscosity cluster, the observed deviations range from +16.2% to +20.5% at 263 K and from +4.1% to +5.8% at 373 K.

CONCLUSIONS

In this work, thermophysical property measurements for 11 blends of the rocket propellant RP-1 have been presented. Specifically, ambient pressure density and speed of sound data, along with the derived property of adiabatic compressibility, were reported over the temperature range of 278 to 343 K. In addition, ambient pressure dynamic and kinematic viscosities over the temperature range of 263 to 373 K were also reported. These measurements were part of a larger study that includes previously reported[9] distillation curve results and detailed compositional analyses.

Different, yet considerable, degrees of variability over the 11 RP-1 samples were observed for all reported properties, with viscosity exhibiting the largest variability. Specifically, over the temperature range 278 to 343 K, density, speed of sound, and adiabatic compressibility varied by 1.3% to 1.4%, 0.6% to 0.8%, and 2.5% to 2.8%, respectively, while viscosity varied by 14.1% to 6.2% over the temperature range 263 to 373 K. Although the 11 samples measured in this study were specially formulated to represent a range of possible recipes, the degree of observed variability is significant, particularly since RP-1 is a fuel with relatively stringent specifications. In addition to comparing the

dx.doi.org/10.1021/ef3004009 | Energy Fuels 2012, 26, 4383−4394

11 RP-1 samples among one another, the measurement results were also compared with previously reported data[18] for another RP-1 sample, RP-1 4572, and with the RP-1 surrogate mixture model[19] that was developed with the aid of that RP-1 4572 data. It is clear from those comparisons that the RP-1 model currently does not represent the degree of variability that may be possible for this fuel. Furthermore, there were discrepancies observed between the model and the measured temperature dependence of certain properties, viscosity in particular. These conclusions were echoed by Lovestead et al.[9] whose distillation results also showed discrepancies when compared to the RP-1 model. The measurement results indicate that the development of a more general model is warranted.

AUTHOR INFORMATION

Corresponding Author

*Phone: 1-303-497-3522. Fax: 1-303-497-5044. E-mail: tfortin@boulder.nist.gov.

Notes

The authors declare no competing financial interest.

ACKNOWLEDGMENTS

The financial support of the Air Force Research Laboratory (Grant MIPR F4FBEX9205G001) is gratefully acknowledged.

REFERENCES

(1) Sutton, G. P. History of liquid propellant rocket engines in the United States. *J. Propul. Power* **2003**, *19*, 978−1007.

(2) Ehricke, K. A. Comparison of propellants and working fluids for rocket propulsion. *J. Am. Rocket Soc.* **1953**, *23*, 287−296.

(3) Edwards, T. Liquid fuels and propellants for aerospace propulsion: 1903−2003. *J. Propul. Power* **2003**, *19*, 1089−1107.

(4) Sutton, G. P. *Rocket Propulsion Elements: An Introduction to the Engineering of Rockets*, 6th ed.; Wiley: New York, 1992.

(5) Detail Specification Propellant, Rocket Grade Kerosene, MIL-DTL-25576E, April 14, 2006.

(6) Bruno, T. J.; Billingsley, M.; Bates, R. W. Findings and recommendations from the joint NIST/AFRL workshop on rocket propellants and hypersonic vehicle fuels, National Institute of Standards and Technology: Boulder, CO, 2008.

(7) Huber, M. L.; Lemmon, E. W.; Bruno, T. J. Effect of RP-1 compositional variability on thermophysical properties. *Energy Fuels* **2009**, *23*, 5550−5555.

(8) Ott, L. S.; Hadler, A. B.; Bruno, T. J. Variability of the rocket propellants RP-1, RP-2, and TS-5: Application of a composition- and enthalpy-explicit distillation curve method. *Ind. Eng. Chem. Res.* **2008**, *47*, 9225−9233.

(9) Lovestead, T. M.; Windom, B. C.; Riggs, J. R.; Nickell, C.; Bruno, T. J. Assessment of the compositional variability of RP-1 and RP-2 with the advanced distillation curve approach. *Energy Fuels* **2010**, *24*, 5611−5623.

(10) Bruno, T. J.; Svoronos, P. D. N. *CRC Handbook of Fundamental Spectroscopic Correlation Charts*; Taylor and Francis CRC Press: Boca Raton, FL, 2005.

(11) Bruno, T. J.; Svoronos, P. D. N., *CRC Handbook of Basic Tables for Chemical Analysis*, 3rd ed.; Taylor and Francis CRC Press: Boca Raton, FL, 2010.

(12) Bruno, T. J.; Smith, B. L. Improvements in the measurement of distillation curves. 2. Application to aerospace/aviation fuels RP-1 and S-8. *Ind. Eng. Chem. Res.* **2006**, *45*, 4381−4388.

(13) Lovestead, T. M.; Bruno, T. J. A comparison of the hypersonic vehicle fuel JP-7 to the rocket propellants RP-1 and RP-2 with the advanced distillation curve method. *Energy Fuels* **2009**, *23*, 3637−3644.

(14) Whetstone, J. R.; Trahey, N. M. *Certificate of Analysis - Standard Reference Material 211d*; National Institute of Standards and Technology: Gaithersburg, MD, 2011; https://www-s.nist.gov/srmors/view_cert.cfm?srm=211D.

(15) Fortin, T. J.; Laesecke, A.; Freund, M.; Outcalt, S. Advanced calibration, adjustment, and operation of a density and sound speed analyzer. *J. Chem. Thermodyn.* **2012**, submitted.

(16) Laesecke, A.; Fortin, T. J.; Splett, J. D. Density, speed of sound, and viscosity measurements of reference materials for biofuels. *Energy Fuels* **2012**, *26*, 1844−1861.

(17) International Organization for Standardization (ISO). *Guide to the Expression of Uncertainty in Measurement*; ISO: Geneva, Switzerland, 1995.

(18) Outcalt, S. L.; Laesecke, A.; Brumback, K. J. Thermophysical properties measurements of rocket propellants RP-1 and RP-2. *J. Propul. Power* **2009**, *25*, 1032−1040.

(19) Huber, A. L.; Lemmon, E. W.; Ott, L. S.; Bruno, T. J. Preliminary surrogate mixture models for the thermophysical properties of rocket propellants RP-1 and RP-2. *Energy Fuels* **2009**, *23*, 3083−3088.

(20) Lemmon, E. W.; Huber, M. L.; McLinden, M. O. *NIST Standard Reference Database 23: Reference Fluid Thermodynamic and Transport Properties (REFPROP), 9.0*; National Institute of Standards and Technology: Gaithersburg, MD, 2010; http://www.nist.gov/srd/nist23.cfm.